HHS Public Access

Author manuscript

Prostaglandins Other Lipid Mediat. Author manuscript; available in PMC 2020 April 01.

Published in final edited form as:

Prostaglandins Other Lipid Mediat. 2019 April ; 141: 40–48. doi:10.1016/j.prostaglandins.2019.02.005.

Quantifying 1-deoxydihydroceramides and 1-deoxyceramides in mouse nervous system tissue

Nicholas U. Schwartz, **Izolda Mileva**, **Mikhail Gurevich**, **Justin Snider**, **Yusuf A. Hannun**, and **Lina M. Obeid**

Health Science Center, L-4, 179, Stony Brook University Medical Center, Stony Brook, NY, 11794-8430, United States

Abstract

Accumulation of deoxysphingolipids (deoxySLs) has been implicated in many neural diseases, although mechanisms remain unclear. A major obstacle limiting understanding of deoxySLs has been the lack of a method easily defining measurement of deoxydihydroceramide (deoxydhCer) and deoxyceramide (deoxyCer) in neural tissues. Furthermore, it is poorly understood if deoxySLs accumulate in the nervous system with aging. To facilitate investigation of deoxydhCer and deoxyCer in nervous system tissue, we developed a method to evaluate levels of these lipids in mouse brain, spinal cord, and sciatic nerve. Many deoxydhCers and brain C24-deoxyCer were present at 1, 3, and 6 months of age. Furthermore, while ceramide levels decreased with age, deoxydhCers increased in sciatic nerve and spinal cord, suggesting they may accumulate in peripheral nerves. C22-deoxydhCer was the highest deoxydhCer species in all tissues, suggesting it may be important physiologically. The development of this method will facilitate straightforward profiling of deoxydhCers and deoxyCers and the study of their metabolism and function. These results also reveal that deoxydhCers accumulate in peripheral nerves with normal aging.

Keywords

deoxysphingolipids; 1-deoxysphingolipids; deoxyceramide; deoxyceramide; lipidomics

1. Introduction

While extensive study has linked sphingolipid dysfunction to many cancers, inflammatory diseases, and aging, one remarkable recent discovery in sphingolipid research involved a rare inherited neuropathy. Hereditary and Sensory Neuropathy 1 (HSAN1), a well-known

To whom correspondence should be addressed: Dr. Lina M. Obeid Health Science Center, L-4, 179, Stony Brook University Medical Center, Stony Brook, NY 11794-8430, Lina.Obeid@stonybrookmedicine.edu.

Author Contributions: NUS, IM, YAH, and LMO designed experiments. NUS, IM, and MG performed experiments. NUS, JS, and IM analyzed data. NUS, IM, and LMO wrote the manuscript.

The authors declare no actual nor potential conflicts of interest.

peripheral neuropathy predominantly causing sensory loss and painful burning in the limbs, was discovered to result from mutations in either the SPTLC1 or SPTLC2 subunits of serine palmitoyltransferase (SPT) (Bejaoui et al., 2001; Dawkins et al., 2001; Murphy et al., 2013; Rotthier et al., 2010). SPT is the preliminary and rate-limiting enzyme in the *de novo* pathway of ceramide genesis, responsible for typically condensing serine and palmitoyl-CoA to produce 3-ketodihydrosphingosine. The discovered mutations altered the substrate specificity of SPT, increasing its incorporation of alanine in lieu of serine, thereby increasing production of deoxySL (deoxysphingolipid) species such as deoxydihydroceramides (deoxydhCers), deoxyceramides (deoxyCers) and deoxysphingoid base species (Gable et al., 2010; Hornemann et al., 2008; Penno et al., 2010; Rotthier et al., 2012; Zitomer et al., 2009) (Fig. 1).[1]One of these deoxysphingoid bases, deoxysphinganine (deoxySA), accumulates in both HSAN1 cellular models and patient plasma samples, causing neurotoxity by interfering with the formation and development of neurites (Penno et al., 2010).

The loss of the C_1-hydroxyl group in these molecules is responsible for altering their structural, metabolic, and functional properties. Absence of this polar hydroxyl group near the end of the sphingoid chain further augments the nonpolar nature of their associated ceramides, which may result in altering their biophysical properties in membranes. Furthermore, the absence of the 1-hydroxyl group prevents the addition of phosphate, phosphocholine, and glycose head groups which are required for the formation of the sphingoid and ceramide phosphates, sphingomyelin (SM), and galactosyl- and glucosylceramides, respectively (Jimenez-Rojo et al., 2014). Thus, the presence of deoxySLs is restricted to the sphingoid bases and the various ceramides. However, while such deoxySL species have long been known to exist in many plants and animal species (Pruett et al., 2008), the physiological and pathological roles of deoxySLs in mammals, especially the nervous system, are still prime for exploration.

Most research on the toxicity of deoxySLs to date has focused on deoxysphingoid bases, although increasing evidence has linked deoxydhCers and deoxyCers to the nervous system, particularly their accumulation in pathological states. C24:1-deoxyCer, along with C24-Cer and many SM species, were found to be reduced in the serum of ADHD patients (Henriquez-Henriquez et al., 2015). Furthermore, increases in deoxySLs such as C24 and C22:1-deoxyCer and C22:1 and C18:1-deoxydhCer have been correlated with the progression of neuropathy in breast cancer patients treated with paclitaxel, a chemotherapeutic with dose-limiting peripheral neuropathy (Kramer et al., 2015). DeoxySA demonstrates concentration dependent neurotoxic effects on primary neurons, particularly those that are aged, that are thought to be due to excessive activation of N-methyl-d-aspartate (NMDA), likely through direct or indirect interaction with the NMDA receptor. While this functional interaction and the responsible receptor subunits still need to be further explored, based on a rescue of deoxySA-induced toxicity from inhibition of ceramide synthases with fumonisin B1, these effects are thought to be due to increased deoxyCer levels (Güntert et al., 2016).

While deoxySLs have been profiled in cells lines such as mouse embryonic fibroblasts (Alecu et al., 2016), they have not been carefully characterized in nervous system tissue, despite many studies implicating their dysregulation in neural disease states. Studies that

have used brain, spinal cords, and sciatic nerves of HSAN mutant mice to examine deoxySLs in the nervous system have mostly focused on measuring deoxysphingoid bases such as deoxySA and deoxysphingosine (deoxySO) and found accumulation of these species in sciatic nerve tissue in the disease state (Eichler et al., 2009; Garofalo et al., 2011). It has been suggested that deoxySA and its associated deoxydhCers are more likely to result in neuronal toxicity than deoxySO and its associated deoxyCers, although extensive evidence to support this claim is lacking (Garofalo et al., 2011). Likewise, many studies have not yet analyzed the full spectrum of acyl chain lengths of deoxyCer and deoxydhCer species (Bertea et al., 2010; Henriquez-Henriquez et al., 2015), and have measured these species in plasma (Bertea et al., 2010; Henriquez-Henriquez et al., 2015; Kramer et al., 2015), cells (Kramer et al., 2015), or using brain tissue (Esaki et al., 2015).

In this study, we sought to develop an efficient and accurate method of reliably measuring and determining the accumulation deoxySL species in neural tissues. To encompass a diverse range of tissue types in the central and peripheral nervous systems that can be relatively easily isolated and probed, we chose to analyze mouse brain, spinal cord, and sciatic nerve tissue. We used time points of 1 month, 3 months, and 6 months for sets of male and female mice in order to track the effect of age and potential gender differences. Indeed, we were able to reliably measure many specific deoxySL species in these tissue samples. The method was able to accurately measure C24-deoxyCer in brain as well as a variety of deoxydhCer species in brain, spinal cord, and sciatic nerve, most predominantly C22-deoxydhCer. The results revealed a trend of increased total deoxydhCers most noticeably in sciatic nerve in 6 month old mice, suggesting that these species may progressively accumulate in peripheral tissue. This method will facilitate straightforward profiling of deoxyCers and deoxydhCer in many neural model mouse systems.

2. Materials and Methods

2.1 Lipid Analysis.

Protein levels of tissue samples and subcellular fractions were measured and the final results were normalized to total protein content. Samples were fortified with an internal standard mix and lipids were extracted twice with a mixture of Ethyl acetate: Isopropanol: Water - 60 : 28 : 12%, as previously described (Bielawski et al., 2006). Sequential, double extraction was performed with two extracts, 2 mL each, that were added together and dried down under nitrogen. The samples were resuspended in 150 uL of Mobile phase B (Methanol:1mM Ammonium formate:0.2% Formic acid). High performance liquid chromatography and mass spectroscopy (HPLC/MS) of ceramide species were performed by the Lipidomics Core at Stony Brook University as previously described (Bielawski et al., 2006).

Mass spectroscopy analyses were conducted on TSQ Quantum Ultra triple quad mass spectrometer with a HESI probe and Accela 1250 HPLC system utilizing positive ionization in MRM mode. The lipids were separated on a Peek Scientific C-8CR column (3 μm particle, 4.6 × 150 mm) and injected into the mass spectrometer, where they were separated and characterized according to their mass-to-charge ratio. The mass spectrometer settings were as follows: spray voltage 3800 V; vaporizer temperature 400°C; sheath gas pressure 60

AU; ion sweep gas 0; capillary temperature 300°C; skimmer offset 0 volts; collision pressure 1.5 mTorr.

The MRM transitions that were used are shown in Fig. 2A. The collision energy was optimized with standard species (see Fig. 2A). RT linear regression analysis was performed to confirm the identify of species which do not have standards. We found a linear relationship between the carbon number and elution times for regular ceramides that we do have standards for. We assumed that the deoxyCers elute in the same way as they are structurally similar and exhibit the similar polarity. The deoxyCers elute 1.05 minutes after ceramides and the deoxydhCers SA elute 1.47 minutes after.

All standards were purchased from Avanti. C16-deoxyCer, C16-deoxydhCer, C24:1-deoxyCer and C24:1-deoxydhCer standards were used for optimization of the MS transitions and all other MS parameters (Fig. 2B). Barring synthesis of standards to assure quality, which would take a significant amount of time and resource, no standards are available for the different deoxydhCers and deoxyCers of interest. Therefore, the conclusions for this study were drawn based on the use of the available reagents (Avanti). Using these standards, as well as all standards for regular ceramides, retention times (RTs) were calculated for C12, C14, C18, C18:1, C20, C20:1, C22, C22:1, C26, and C26:1 deoxyCer and deoxydhCer. The deoxy species for which no standards were available were quantified utilizing surrogate calibration curves produced by the closest sphingolipid counterpart that had available standards.

To verify the identity of the aforementioned lipids, we manually inspected peaks produced at the correct mass and predicted retention time. Representative peaks for C24-deoxydhCer and C22-deoxydhCer demonstrated relatively high peak intensity with little background signal (Fig. 3A–B). Thus, these peaks can be designated as deoxydhCers and further quantified by calculating the area under the curve with high confidence. Samples were spiked with a low level of standards to ensure correct assigning of the peaks. To further verify the identity designated to these detected entities, we inspected calibration curves to ensure linearity. Calibration curves for C16-deoxydhCer, C24:1-deoxydhCer, C16-deoxyCer, and C24:1-deoxyCer demonstrated high linearity, further validating the use of these parameters to identify these molecules (Fig. 3C–F).

We determined the LOD and LOQ of the method using low quantities of the standards (Supplementary Fig. 1A–B). To further validate the reproducibility of the method, we injected a control sample of known amount for ten consecutive days, demonstrating strong precision (Supplementary Fig. 1C). We also validated the recovery and extraction efficiency by determining the recovery of 50 pmol/mL standard from seven samples (Supplementary Fig. 1D).

2.2 Mouse Tissue

All animal procedures were approved by the Stony Brook University Institutional Animal Care and Use Committee (IACUC) and followed the guidelines of the American Veterinary Medical Association. Brain, spinal cord, sciatic nerves from WT C57B6 mice were dissected and flash frozen in liquid nitrogen and later homogenized in 20 mM Tris Buffer pH 7.8

using a QIAGEN TissueRuptor. Samples were centrifuged for 3 min at 500 xg and the supernatant was collected. Protein measurements were used for normalization of lipid levels.

2.3 Statistical Analysis

Kruskal-Wallis tests were used to compare measurements of lipid species at 1 month, 3 months and 6 months of age because of small sample size (6 mice in each individual group) and violations in the normality assumption. No multiple testing adjustment was implemented here because of exploratory nature in our experiments and hence all unadjusted p-values are reported (Bender and Lange, 2001). Statistical significance level was set at 0.05 and analysis was performed using SAS 9.4 (SAS Institute Inc., Cary, NC). A positive test signifies that there are statistically significant differences between at least two of the groups tested. Error bars represent Standard Error from each group (n=6).

3. Results

3.1 Parameters for deoxyCer measurements

We set out to measure deoxysphingoid, deoxydhCer, and deoxyCer species produced from alanine and palmitoyl-CoA in *de novo* synthesis. C16 and C24:1 deoxydhCer and deoxyCer standards were used to determine parameters for accurately measuring deoxydhCer and deoxyCer species. Using these standards, we were able to calculate the parameters for measuring C12, C14, C18, C18:1, C20, C20:1, C22, C22:1, C26, and C26:1 deoxydhCers and deoxyCers. Precursor ion peak, product ion peak, collision energy, and retention time for all these species are listed (Fig. 2A). To empirically determine these “target” values, we used specific source curves from standards and previously identified species (Fig. 2B).

3.2 Deoxysphingoid bases are largely unaltered with age

Brain, spinal cord, and sciatic nerve dissected and flash frozen from mice were chosen as relevant models to represent a diversity of neuronal tissues. Results from analysis of brain, spinal cord, and sciatic nerve were analyzed at ages of 1, 3, and 6 months. Males and females did not show large changes in any lipid species analyzed (data not shown). To increase the power of comparisons, data from males and females were grouped together and stratified by age to identify alterations in deoxySL species during nervous system development as mice reached adulthood. We considered the general similarity of male and female mouse data as further validity of our method of quantification. Sphingolipid species that were below the limit of quantification in many samples or those that did not possess symmetrical peaks clearly distinct from background signal on analysis of LC/MS data were not included in the analysis of the data. This ensures that displayed data represent true peaks identifying deoxySL species. The data generated demonstrated many interesting trends, despite only using six mice from each age group as was originally designed to validate this method.

As such, we initially analyzed sphingoid and deoxysphingoid bases in all tissues, as has been done previously (Fig 4) (Bielawski et al., 2006). Notably, deoxySO levels were below the limit of quantification in all three tissues. DeoxySA was below quantification in sciatic nerve but was observed in brain and spinal cord tissue; however, deoxySA was not altered

with increased age in spinal cord tissue. Similarly, sphingosine levels were relatively stable with increased age. Sphinganine, however, demonstrated an age-related decline in both brain and sciatic nerve but was not detected in spinal cord. Additionally, greater levels of sphingosine than sphinganine were observed in all tissues. In contrast deoxySA was much higher than deoxySO in brain and spinal cord. Taken together, these data reveal detectable levels of deoxySA but lack of accumulation of deoxySO.

Next, we analyzed the levels of ceramide and dhCer. Mouse embryonic fibroblast cells show about 10 times greater ceramide levels than dhCer (Siddique et al., 2013). To validate these results in a neuronal model, we measured ceramide and dhCer species using HT-22 cells, an immortalized cell line derived from mouse hippocampal cells. HT-22 cells demonstrated approximately a 25 times increase of ceramide compared to dhCer, and large increases in ceramide were consistent for every species in which dhCer was quantifiable (data not shown). As a confirmatory measure, we measured C16-Cer and C16-dhCer levels in nervous system tissues. Consistently, C16-Cer was much more abundant than C16-dhCer. Ceramides demonstrated approximately 100 times, 10 times, and 15 times increases in brain, spinal cord, and sciatic nerve tissue, respectively, and demonstrated similar trends as dhCers (Supplementary Fig. 2). As such, consistent with the established view of *de novo* sphingolipid metabolism, we determined that dhCers in these tissues are predominantly converted to ceramides (Hannun and Obeid, 2017).

3.3 DeoxydhCers are abundant and increase with age in spinal cord and sciatic nerve

Since much less is known about deoxydhCer and deoxyCer species, it was necessary to accurately quantify levels of both. Only one species of deoxyCer was sufficiently present in tissue for accurate quantification—C24-deoxyCer in the brain (Supplementary Fig. 3). Interestingly, while this species was much less abundant than C24-Cer, it appeared to slightly rise with increased age in contrast to C24-Cer which sharply decreased. This suggests that C24-deoxyCer may serve an important role in aging in the brain.

Importantly, there was a general trend of decreased ceramide levels between 1 and 6 month old mice in each tissue (Fig. 5). Similarly, brain tissue also demonstrated a decrease in deoxydhCers that appeared to be even slightly sharper than the decrease in ceramides in the brain. Interestingly, however, deoxydhCers appeared to potentially increase in the spinal cord and significantly increase in the sciatic nerve with increasing age. This was especially stark in the sciatic nerve, with almost a doubling in total deoxydhCer content between 1 and 6 month old mice, despite the overall trend of decreased ceramides between these two timepoints. This suggests that in peripheral nervous system tissue, deoxydhCers may increase with nervous system development, despite decreases in total ceramide levels. Furthermore, total deoxydhCers were especially abundant in peripheral tissue. Sciatic nerve tissue displayed around 100 times increase in deoxydhCers compared to brain, despite sciatic nerve only containing about 5 times as much total deoxydhCer as ceramide. These results suggest that deoxydhCer may increasingly accumulate in the peripheral nervous system.

3.4 C22 is the predominant deoxydhCer in mouse neural tissue

To further investigate these trends in deoxydhCers, we analyzed individual species (Fig. 6). In all three tissue types, C22-deoxydhCer was the most prevalent species. This was especially noticeable in spinal cord tissue, in which C22-deoxydhCer dwarfed the contribution of other deoxydhCer species. Generally, C18 and C24:1 species were next highest in abundance. Generally, the species that were clearly detectable were the longer acyl chain deoxydhCers. C18, C22, C24, and C24:1 were common in all species, with C22:1 also being a minor component present in the brain. Generally, for each species there were similar trends in levels with age. These results suggest that common species of deoxydhCer are present in different types of nervous system tissue and that C22-deoxydhCer may play an important role.

4. Discussion

In this study, we developed a method to accurately determine deoxydhCer and deoxyCer levels in mouse nervous system tissue, given the increasingly suspected importance of these species in nervous system pathology. We used C57B6 mice as an experimental model to demonstrate the presence of deoxySLs in wild-type mice without any manipulation. The method used in this paper makes use of recently available standards using a general mass spectrometry method that has been published for quite some time. Therefore, this demonstrates a feasible method for groups using mouse models of HSAN1, diabetic neuropathy, ADHD, chemotherapeutic treatments implicated in causing neuropathy, or other neural models to evaluate changes in deoxySLs.

A major observation of this study was the much greater quantity and variety of deoxydhCer than deoxyCer in tissue. C24-deoxyCer was the only deoxyCer species detectable above quantification. This is similar to other studies that only detect deoxyCers with very long acyl chains (Alecu et al., 2016). As mouse age increased, this species increased in abundance, whereas C24-Cer notably decreased. This suggests that C24-deoxyCer may play an important role in aging in the nervous system, as its accumulation cannot be directly tied to an increase in non-selective C24 acylation of sphingoid bases. We would hypothesize that this and other trends seen with older mice would be further exaggerated with mice that are greater than 1 year old.

Similar to results published using MEF cells, deoxydhCers are present in greater quantity than deoxyCers (Alecu et al., 2016), suggesting that contrary to most ceramide species, deoxydhCers are not readily desaturated. This suggests that desaturase activity (DES1 and possibly DES2) may have a much greater preference for the dhCers over the deoxydhCers. While formally, the low to undetectable levels of deoxyCers may be due to increased turnover, this is unlikely as none of the known enzymes of ceramide metabolism, save the ceramidases, is capable of acting on the deoxyCers. Ceramidases would produce deoxySO which was very low in our studies. Further supporting this hypothesis, deoxySO is also thought to differ in structure from sphingosine by having distinct placement of the double bond in its sphingoid backbone at the 14 position instead of the 4 position as observed in sphingosine (Steiner et al., 2016). Together, the results support lack of activity of the desaturases on deoxydhCers.

Similar to published distributions of deoxydhCers from cells grown in culture, we observed a relative abundance of C24, C24:1, C18 (but not C16 species) of deoxyCers in all tissue types (Alecu et al., 2016). This suggests that the six distinct CerS may exhibit different preferences for canonical sphingoid bases vs. the deoxysphingoids in catalyzing acyl chain additions. Since C24 and C18 are preferential products of CerS2, CerS4, and CerS1, whereas C16-Cer is formed by either CerS5 or CerS6, these results suggest that the latter two CerSs have very poor action on deoxysphingoid bases.

This study makes clear that wild-type mice produce deoxySLs without perturbation. It is still not well understood if these deoxySL species serve a structural and/or bioactive role, or if they are byproducts from promiscuous action of SPT due to proximal alanine. Furthermore, deoxydhCers were especially abundant in sciatic nerve tissue compared to that of brain and even spinal cord. It is unknown why deoxydhCer levels are so much higher in peripheral nerves, and if this is due to increased generation or decreased breakdown. The cytochrome P450 4F enzymes were recently shown to be capable of hydroxylating and degrading deoxySL species (Alecu et al., 2017).

Preliminary studies have begun to investigate the biophysical properties and biological functions of deoxySLs. Due to their high hydrophobicity, deoxydhCers and deoxyCers have lower miscibility with SM in bilayers than their non-deoxySL counterparts (Jimenez-Rojo et al., 2014). Potential functional roles include serving as scaffolds for antigen presentation by selectively binding specific cluster of differentiation proteins due to their highly hydrophobic nature (Huang et al., 2011). However, much remains to be discovered about how these molecules may alter membrane properties in different organelles such as endoplasmic reticulum (ER). DeoxySA localizes to Golgi and ER, and can cause ER stress, similar to results seen in HSAN patients, as measured by GADD153 levels and XBP1 splicing (Alecu et al., 2016; Gable et al., 2010; Myers et al., 2014). Furthermore, deoxySA induces mitochondrial fragmentation and dysfunction that precedes axonal degeneration, although the effects of deoxyCer and deoxydhCer on mitochondria have not been carefully examined (Alecu et al., 2016). Similar morphological findings have been observed in HSAN patient lymphoblasts (Myers et al., 2014).

The most immediate application of research on deoxySLs and specifically deoxyCer and deoxydhCer will likely lie in understanding the pathology and developing treatments for HSAN1. HSAN1 is typically inherited in an autosomal dominant fashion, suggesting that deoxySL accumulation may lead to toxicity in a dominant-negative fashion and may be modulated by availability of reactants. Expression of HSAN1 mutants in yeast cells suggest that disease mutants may not directly affect the binding site but more efficiently allow bound alanine to react with acyl-CoA substrates (Gable et al., 2010). Experiments observing beneficial and detrimental effects of serine and alanine, respectively, on deoxySL reduction and HSAN symptoms have been extended to preliminary trials on humans with promising results of decreased deoxySLs in serine supplemented diets (Auranen et al., 2017; Eichler et al., 2009; Fridman et al., 2017; Garofalo et al., 2011). Furthermore, increases in neurite length and p-ERM expression from DRGs of HSAN mutant mice were lost with administration of serine or removal of alanine (Jun et al., 2015).

DeoxySLs have further been suggested to play a role in the pathology of many other diseases, such as diabetes mellitus. Diabetic neuropathy presents similarly to HSAN1 with late and insidious loss of peripheral nerve function, especially sensory modalities. Multiple studies have suggested that serum from patients with type 2 diabetes contains increased deoxySO and deoxySA, potentially due to an increased alanine:serine ratio as observed in patient plasma (Bertea et al., 2010; Wei et al., 2014). Increased deoxySLs have also been observed in patients with metabolic syndrome, although type 2 diabetics do not present with significantly different levels, potentially limiting the use of deoxySLs use as a biomarker of disease progression (Othman et al., 2012). Further evidence suggests many deoxyCer species are increased in diabetic patients (Kramer et al., 2015). Interestingly, while deoxySL levels have not been associated with type 1 diabetes (Wei et al., 2014), type 1 diabetic patients exhibiting peripheral neuropathy demonstrated increased C24-deoxyCer, along with C24 and C26 ceramides (Hammad et al., 2016).

DeoxySA has been carefully studied as a potential anti-cancer therapeutic, although it has failed to show significant promise in early clinical trials. Originally isolated from the clam, *Mactromeris polynyma*, deoxySA, also known as spisulosine or ES-285, decreased cell growth, prevented stress fiber formation, and increased apoptotic signaling by activation of caspases 3 and 12 and modifying p53 phosphorylation, and induced *de novo* ceramide production (Cuadros et al., 2000; Salcedo et al., 2007; Sánchez et al., 2008). However, phase I clinical trials demonstrated that deoxySA administration to patients with advanced solid tumors was linked to dose-limiting neuro- and hepatotoxicities and pyrexia with often mild to unobservable objective anti-cancer effects, resulting in its discontinuation (Baird et al., 2009; Massard et al., 2012; Schöffski et al., 2011; Vilar et al., 2012). Given their neurotoxicity *in vitro*, deoxydhCers and deoxyCers may also demonstrate clinical side effects, but their effectiveness as chemotherapeutics is unknown.

5. Conclusions

We have developed a novel method for accurately determining deoxydhCer and deoxyCer levels in brain, spinal cord, and sciatic nerve of mice. Data suggests that deoxydhCers accumulate in peripheral nervous tissue with aging and that C22-deoxydhCer is highly produced throughout the nervous system. This method will facilitate efficient screening and determination of deoxyCer and deoxydhCer levels in many mouse models of neural disease and dysfunction, providing us with a better understanding of the pathophysiology of deoxySLs in the nervous system.

Supplementary Material

Refer to Web version on PubMed Central for supplementary material.

Acknowledgements

We thank the Stony Brook Lipidomics Core for measurement and analysis of sphingolipids and Dr. Ashley Snider for assistance in managing mice. We acknowledge the biostatistical consultation and analysis provided by Dr. Jie Yang, Lizhou Nie and the Biostatistical Consulting Core at School of Medicine, Stony Brook University. Funding: This work was supported by the National Institute of Health grants GM062887 and Veterans Affairs Merit Award to LMO.

Glossary

deoxyCer	1-deoxyceramide
deoxydhCer	1-deoxydihydroceramide
deoxySA	1-deoxysphinganine
deoxySL	1-deoxysphingolipid
deoxySO	deoxysphingosine
DES	sphingolipid delta(4)-desaturase
dhCer	dihydroceramide
HPLC/MS	High performance liquid chromatography and mass spectroscopy
HSAN	hereditary sensory and autonomic neuropathy
NMDA	N-methyld-aspartate
RT	retention time
SM	sphingomyelin

References

Alecu I, Othman A, Penno A, Saied EM, Arenz C, Von Eckardstein A Hornemann T, 2017 Cytotoxic 1-deoxysphingolipids are metabolized by a cytochrome P450-dependent pathway. J. Lipid Res. 58, 60–71. 10.1194/jlr.M072421 [PubMed: 27872144]

Alecu I, Tedeschi A, Behler N, Wunderling K, Lauterbach MAR, Gaebler A, Ernst D, Van Veldhoven PP Al-amoudi A, Latz E, Othman A, Kuerschner L, Hornemann T, 2016 Localization of 1-deoxysphingolipids to mitochondria induces mitochondrial dysfunction. J. Lipid Res. 58, 42–59. 10.1194/jlr.M068676 [PubMed: 27881717]

Auranen M, Toppila J, Suriyanarayanan S, Lone MA, Paetau A, Tyynismaa H, Hornemann T, Ylikallio E, 2017 Clinical and metabolic consequences of L-serine supplementation in hereditary sensory and autonomic neuropathy type 1C. Cold Spring Harb Mol Case Stud 3, 1–8. 10.1101/mcs.a002212

Baird RD, Kitzen J, Clarke PA, Planting A, Reade S, Reid A, Welsh L, Lopez Lazaro L, de las Heras B, Judson IR, Kaye SB, Eskens F, Workman P, deBono JS, Verweij J, 2009 Phase I safety, pharmacokinetic, and pharmacogenomic trial of ES-285, a novel marine cytotoxic agent, administered to adult patients with advanced solid tumors. Mol. Cancer Ther. 8, 1430–1437. 10.1158/1535-7163.MCT-08-1167 [PubMed: 19509256]

Bejaoui K, Wu C, Scheffler MD, Haan G, Ashby P, Wu L, de Jong P, Brown RH Jr., 2001 SPTLC1 is mutated in hereditary sensory neuropathy, type 1. Nat. Genet 27, 261–262. 10.1038/85817 [PubMed: 11242106]

Bender R, Lange S, 2001 Adjusting for multiple testing - When and how? J. Clin. Epidemiol 54, 343–349. 10.1016/S0895-4356(00)00314-0 [PubMed: 11297884]

Bertea M, Rütti MF, Othman A, Marti-Jaun J, Hersberger M, von Eckardstein A, Hornemann T, 2010 Deoxysphingoid bases as plasma markers in diabetes mellitus. Lipids Health Dis. 9, 84 10.1186/1476-511X-9-84 [PubMed: 20712864]

Bielawski J, Szulc ZM, Hannun YA, Bielawska A, 2006 Simultaneous quantitative analysis of bioactive sphingolipids by high-performance liquid chromatography-tandem mass spectrometry. Methods 39, 82–91. 10.1016/j.ymeth.2006.05.004 [PubMed: 16828308]

Cuadros R, Montejo De Garcini E, Wandosell F, Faircloth G, Fernández-Sousa JM, Avila J, 2000 The marine compound spisulosine, an inhibitor of cell proliferation, promotes the disassembly of actin stress fibers. Cancer Lett. 152, 23–29. 10.1016/S0304-3835(99)00428-0 [PubMed: 10754202]

Dawkins JL, Hulme DJ, Brahmbhatt SB, Auer-grumbach M, Nicholson GA, 2001 Mutations in SPTLC1, encoding serine palmitoyltransferase, long chain base subunit-1, cause hereditary sensory neuropathy type I. Nat. Genet 27, 309–312. [PubMed: 11242114]

Eichler FS, Hornemann T, McCampbell A, Kuljis D, Penno A, Vardeh D, Tamrazian E, Garofalo K, Lee H-J, Kini L, Selig M, Frosch M, Gable K, von Eckardstein A, Woolf CJ, Guan G, Harmon JM, Dunn TM, Brown RH, 2009 Overexpression of the wild-type SPT1 subunit lowers desoxysphingolipid levels and rescues the phenotype of HSAN1. J. Neurosci 29, 14646–51. 10.1523/JNEUROSCI.2536-09.2009 [PubMed: 19923297]

Esaki K, Sayano T, Sonoda C, Akagi T, Suzuki T, Ogawa T, Okamoto M, Yoshikawa T, Hirabayashi Y, Furuya S, 2015 L-serine deficiency elicits intracellular accumulation of cytotoxic deoxysphingolipids and lipid body formation. J. Biol. Chem 290, 14595–14609. 10.1074/jbc.M114.603860 [PubMed: 25903138]

Fridman V, Novak P, David W, Macklin E, McKenna-Yasek D, Walsh K, Oaklander AL, Brown R, Hornemann T, Eichler F, 2017 A randomized, double-blind, placebo-controlled, delayed-start trial to evaluate the safety and efficacy of l-serine in subjects with hereditary sensory and autonomic neuropathy type 1 (HSAN1) (s45.001). Neurology 88.

Gable K, Gupta SD, Han G, Niranjanakumari S, Harmon JM, Dunn TM, 2010 A disease-causing mutation in the active site of serine palmitoyltransferase causes catalytic promiscuity. J. Biol. Chem 285, 22846–22852. 10.1074/jbc.M110.122259 [PubMed: 20504773]

Garofalo K, Penno A, Schmidt BP, Lee HJ, Frosch MP, Von Eckardstein A, Brown RH, Hornemann T, Eichler FS, 2011 Oral L-serine supplementation reduces production of neurotoxic deoxysphingolipids in mice and humans with hereditary sensory autonomic neuropathy type 1. J. Clin. Invest 121, 4735–4745. 10.1172/JCI57549 [PubMed: 22045570]

Güntert T, Hänggi P, Othman A, Suriyanarayanan S, Sonda S, Zuellig RA, Hornemann T, Ogunshola OO, 2016 1-Deoxysphingolipid-induced neurotoxicity involves N-methyl-D-aspartate receptor signaling. Neuropharmacology 110, 211–222. 10.1016/j.neuropharm.2016.03.033 [PubMed: 27016021]

Hammad SM, Baker NL, El Abiad JM, Spassieva SD, Pierce JS, Rembiesa B, Bielawski J, Lopes-Virella MF, Klein RL, 2016 Increased Plasma Levels of Select Deoxy-ceramide and Ceramide Species are Associated with Increased Odds of Diabetic Neuropathy in Type 1 Diabetes: A Pilot Study. NeuroMolecular Med. 10.1007/s12017-016-8423-9

Hannun YA, Obeid LM, 2017 Sphingolipids and their metabolism in physiology and disease. Nat. Rev. Mol. Cell Biol. 10.1038/nrm.2017.107

Henriquez-Henriquez MP, Solari S, Quiroga T, Kim BI, Deckelbaum RJ, Worgall TS, 2015 Low serum sphingolipids in children with attention deficit-hyperactivity disorder. Front. Neurosci 9, 1–9. 10.3389/fnins.2015.00300 [PubMed: 25653585]

Hornemann T, Penno A, von Eckardstein A, 2008 The accumulation of two atypical sphingolipids cause hereditary sensory neuropathy type 1 (HSAN1). Chem. Phys. Lipids 154, S62 10.1016/j.chemphyslip.2008.05.169

Huang S, Cheng T-Y, Young DC, Layre E, Madigan CA, Shires J, Cerundolo V, Altman JD, Moody DB, 2011 Discovery of deoxyceramides and diacylglycerols as CD1b scaffold lipids among diverse groove-blocking lipids of the human CD1 system. Proc. Natl. Acad. Sci. U. S. A 108, 19335–40. 10.1073/pnas.1112969108 [PubMed: 22087000]

Jimenez-Rojo N, Sot J, Busto JV, Shaw WA, Duan J, Merrill AH, Alonso A, Goni FM, 2014 Biophysical Properties of Novel 1-Deoxy-(Dihydro)ceramides Occurring in Mammalian Cells. Biophys. J 107, 2850–2859. 10.1016/j.bpj.2014.10.010 [PubMed: 25517151]

Jun BK, Chandra A, Kuljis D, Schmidt BP, Eichler FS, 2015 Substrate Availability of Mutant SPT Alters Neuronal Branching and Growth Cone Dynamics in Dorsal Root Ganglia. J. Neurosci 35, 13713–9. 10.1523/JNEUROSCI.1403-15.2015. [PubMed: 26446223]

Kramer R, Bielawski J, Kistner-Griffin E, Othman A, Alecu I, Ernst D, Kornhauser D, Hornemann T, Spassieva S, 2015 Neurotoxic 1-deoxysphingolipids and paclitaxel-induced peripheral neuropathy. FASEB J. 29, 4461–72. 10.1096/fj.15-272567 [PubMed: 26198449]

Massard C, Salazar R, Armand JP, Majem M, Deutsch E, García M, Oaknin A, Fernndez-García EM, Soto A, Soria JC, 2012 Phase i dose-escalating study of ES-285 given as a three-hour intravenous infusion every three weeks in patients with advanced malignant solid tumors. Invest. New Drugs 30, 2318–2326. 10.1007/s10637-011-9772-8 [PubMed: 22215532]

Murphy SM, Ernst D, Wei Y, Laura M, Liu Y, Polke J, Blake J, Winer J, Houlden H, Hornemann T, Reilly MM, 2013 Hereditary sensory and autonomic neuropathy type 1 (HSANI) cased by a novel mutation in SPTLC2. Neurology 80, 2106–2111. [PubMed: 23658386]

Myers SJ, Malladi CS, Hyland R. a, Bautista T, Boadle R, Robinson PJ, Nicholson G. a, 2014 Mutations in the SPTLC1 Protein Cause Mitochondrial Structural Abnormalities and Endoplasmic Reticulum Stress in Lymphoblasts. DNA Cell Biol. 33, 399–407. 10.1089/dna.2013.2182 [PubMed: 24673574]

Othman A, Rütti MF, Ernst D, Saely CH, Rein P, Drexel H, Porretta-Serapiglia C, Lauria G, Bianchi R, von Eckardstein A, Hornemann T, 2012 Plasma deoxysphingolipids: a novel class of biomarkers for the metabolic syndrome? Diabetologia 55, 421–31. 10.1007/s00125-011-2384-1 [PubMed: 22124606]

Penno A, Reilly MM, Houlden H, Laurá M, Rentsch K, Niederkofler V, Stoeckli ET, Nicholson G, Eichler F, Brown RH, von Eckardstein A, Hornemann T, 2010 Hereditary sensory neuropathy type 1 is caused by the accumulation of two neurotoxic sphingolipids. J. Biol. Chem 285, 11178–87. 10.1074/jbc.M109.092973 [PubMed: 20097765]

Pruett ST, Bushnev A, Hagedorn K, Adiga M, Haynes C. a, Sullards MC, Liotta DC, Merrill AH, 2008 Biodiversity of sphingoid bases (“sphingosines”) and related amino alcohols. J. Lipid Res. 49, 1621–1639. 10.1194/jlr.R800012-JLR200 [PubMed: 18499644]

Rotthier A, Auer-Grumbach M, Janssens K, Baets J, Penno A, Almeida-Souza L, Van Hoof K, Jacobs A, De Vriendt E, Vondra P, Schlotter-Weigel B, Lo W, Seeman P, De Jonghe P Van Dijck P, Jordanova A, Hornemann T, Timmerman V, 2010 Mutations in the SPTLC2 Subunit of Serine Palmitoyltransferase Cause Hereditary Sensory and Autonomic Neuropathy Type I. Am. J. Hum. Genet 87, 513–522. 10.1016/j.ajhg.2010.09.010 [PubMed: 20920666]

Rotthier A, Baets J, Timmerman V, Janssens K, 2012 Mechanisms of disease in hereditary sensory and autonomic neuropathies. Nat. Rev. Neurol 8, 73–85. 10.1038/nrneurol.2011.227 [PubMed: 22270030]

Salcedo M, Cuevas C, Alonso JL, Otero G, Faircloth G, Fernandez-Sousa JM, Avila J, Wandosell F, 2007 The marine sphingolipid-derived compound ES 285 triggers an atypical cell death pathway. Apoptosis 12, 395–409. 10.1007/s10495-006-0573-z [PubMed: 17191124]

Sánchez AM, Malagarie-Cazenave S, Olea N, Vara D, Cuevas C, Díaz-Laviada I, 2008 Spisulosine (ES-285) induces prostate tumor PC-3 and LNCaP cell death by de novo synthesis of ceramide and PKCζ activation. Eur. J. Pharmacol 584, 237–245. 10.1016/j.ejphar.2008.02.011 [PubMed: 18343365]

Schöffski P, Dumez H, Ruijter R, Miguel-Lillo B, Soto-Matos A, Alfaro V, Giaccone G, 2011 Spisulosine (ES-285) given as a weekly three-hour intravenous infusion: Results of a phase i dose-escalating study in patients with advanced solid malignancies. Cancer Chemother. Pharmacol 68, 1397–1403. 10.1007/s00280-011-1612-1 [PubMed: 21465314]

Siddique MM, Li Y, Wang L, Ching J, Mal M, Ilkayeva O, Wu YJ, Bay BH, Summers SA, 2013 Ablation of Dihydroceramide Desaturase 1, a Therapeutic Target for the Treatment of Metabolic Diseases, Simultaneously Stimulates Anabolic and Catabolic Signaling. Mol. Cell. Biol 33, 2353–2369. 10.1128/MCB.00226-13 [PubMed: 23547262]

Steiner R, Saied EM, Othman A, Arenz C, Maccarone AT, Poad BLJ, Blanksby SJ, von Eckardstein A, Hornemann T, 2016 Elucidating the chemical structure of native 1-deoxysphingosine. J. Lipid Res. 57, 1194–1203. 10.1194/jlr.M067033 [PubMed: 27165858]

Vilar E, Grünwald V, Schöffski P, Singer H, Salazar R, Iglesias JL, Casado E, Cullell-Young M, Baselga J, Tabernero J, 2012 A phase I dose-escalating study of ES-285, a marine sphingolipid-derived compound, with repeat dose administration in patients with advanced solid tumors. Invest. New Drugs 30, 299–305. 10.1007/s10637-010-9529-9 [PubMed: 20820909]

Wei N, Pan J, Pop-Busui R, Othman A, Alecu I, Hornemann T, Eichler FS, 2014 Altered sphingoid base profiles in type 1 compared to type 2 diabetes. Lipids Health Dis. 13, 161 10.1186/1476-511X-13-161 [PubMed: 25305670]

Zitomer NC, Mitchell T, Voss KA, Bondy GS, Pruett ST, Garnier-Amblard EC, Liebeskind LS, Park H, Wang E, Sulllards MC, Merrill AH, Riley RT, 2009 Ceramide synthase inhibition by fumonisin B1 causes accumulation of 1-deoxysphinganine. A novel category of bioactive 1-deoxysphingoid bases and 1-deoxydihydroceramides biosynthesized by mammalian cell lines and animals. J. Biol. Chem 284, 4786–4795. 10.1074/jbc.M808798200 [PubMed: 19095642]

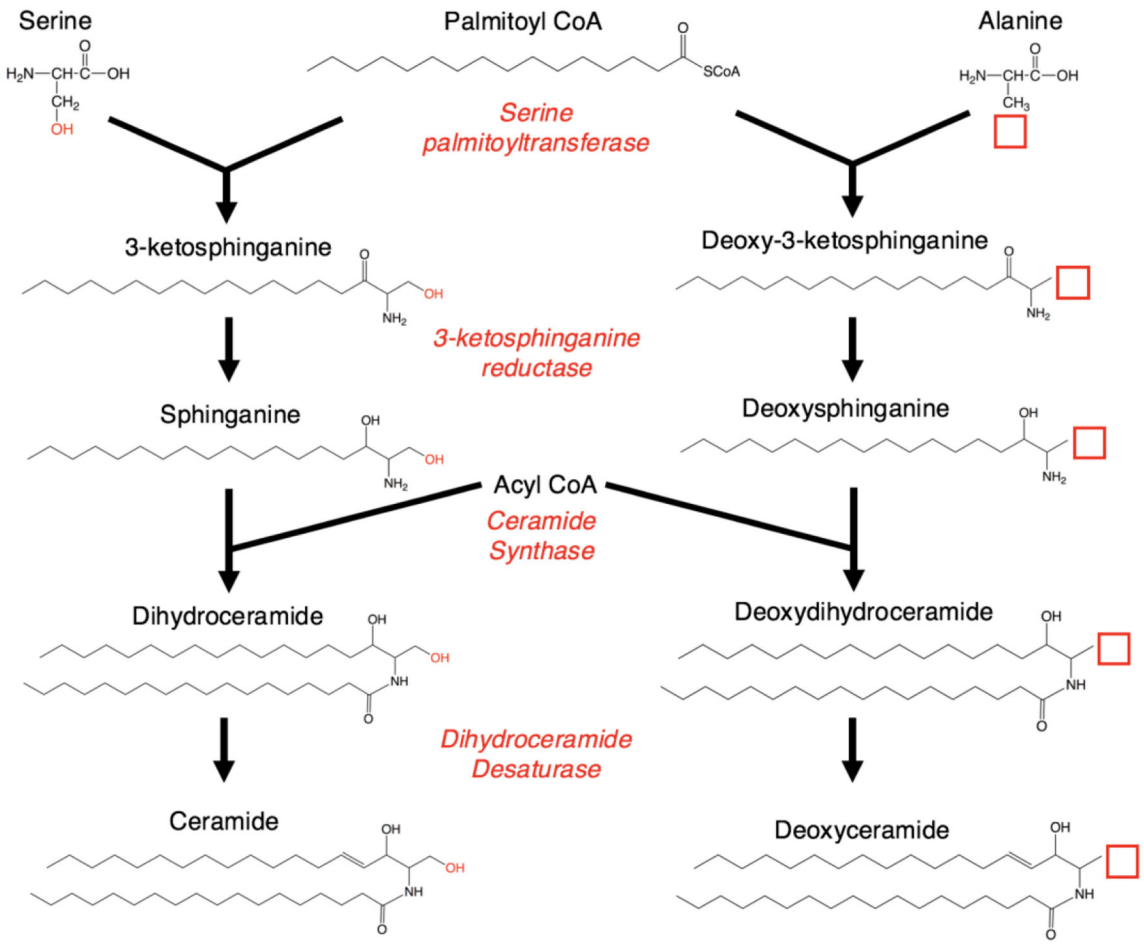

Fig. 1.

Schematic of ceramide synthesis. Serine palmitoyltransferase is responsible for condensing palmitoyl-CoA and serine to generate 3-ketosphinganine, which undergoes further modification by a series of enzymes in the generation of *de novo* ceramide. Incorporation of alanine, which resembles serine but lacks a hydroxyl group, results in the formation of a 1-deoxy-3-ketosphinganine. Despite lacking the 1-hydroxyl at the end of the sphingoid chain, this species is presumably able to undergo modification by other enzymes in the *de novo* pathway of ceramide genesis to create 1-deoxydhCer and 1-deoxyCer.

Properties of Measured Sphingolipid Species

Name	Precursor ion	Product ion	Collision Energy	Retention Time
C12-Cer	482.5	464.2	10	13.49
C14-Cer	510.5	492.6	10	15.49
C16-Cer	538.5	520.6	10	17.00
C18-Cer	566.5	548.6	12	18.50
C18:1-Cer	564.4	546.4	10	17.40
C20-Cer	594.5	576.5	10	20.09
C20:1-Cer	592.5	574.5/264.2	10/25	19.00
C22-Cer	622.5	604.6	12	21.79
C22:1-Cer	620.6	602.6/264.2	10/25	20.29
C24-Cer	650.7	632.6	10	23.62
C24:1-Cer	648.6	630.7	12	22.00
C26-Cer	678.7	660.7	10	25.60
C26:1-Cer	676.8	658.7	12	24.00

Properties of Measured DeoxySL Species

Name	Precursor ion	Product ion	Collision Energy	Retention Time
C12-deoxyCer	466.5	266.2	22	14.50
C12-deoxydhCer	468.6	268.2	22	15.00
C14-deoxyCer	494.5	266.2	22	16.30
C14-deoxydhCer	496.5	268.2	22	17.00
C16-deoxyCer	522.4	266.2	22	17.85
C16-deoxydhCer	524.5	268.2	25	18.50
C18-deoxyCer	550.6	266.2	25	19.30
C18-deoxydhCer	552.6	268.2	22	20.00
C20-deoxyCer	578.6	266.2	22	21.00
C29-deoxydhCer	580.6	268.2	22	21.60
C22-deoxyCer	606.6	266.2	22	22.70
C22-deoxydhCer	608.6	268.2	22	23.30
C24-deoxyCer	634.6	266.2	22	24.40
C24-deoxydhCer	636.6	268.2	22	25.20
C26-deoxyCer	662.6	266.2	22	26.50
C26-deoxydhCer	664.6	268.2	22	27.10
C18:1-deoxyCer	548.6	266.2	25	18.40
C18:1-deoxydhCer	550.5	268.2	25	18.90
C20:1-deoxyCer	576.6	266.2	25	19.90
C20:1-deoxydhCer	578.6	268.2	25	20.50
C22:1-deoxyCer	604.6	266.2	25	21.20
C22:1-deoxydhCer	606.5	268.2	25	21.80
C24:1-deoxyCer	632.6	266.2	25	23.00
C24:1-deoxydhCer	634.7	268.2	25	23.50
C26:1-deoxyCer	660.6	266.2	25	24.80
C26:1-deoxydhCer	662.5	268.2	25	25.50
DeoxySO	284.2	266.2	10	6.20
DeoxySA	286.3	268.2	12	6.40

DeoxySL Species Used for Calculations

Source	Target
C14-Cer	C12-Cer
C18:1-Cer	C20:1-Cer
C24:1-Cer	C22:1-Cer
C24:1-Cer	C26:1-Cer
C24-Cer	C26-Cer
C14-Cer	C12-deoxyCer
C14-Cer	C12-deoxydhCer
C14-Cer	C14-deoxyCer
C14-Cer	C14-deoxydhCer
C16-deoxyCer	C18:1-deoxyCer
C16-deoxydhCer	C18:1-deoxydhCer
C16-deoxyCer	C18-deoxyCer
C16-deoxydhCer	C18-deoxydhCer
C20-Cer	C20:1-deoxyCer
C20-Cer	C20:1-deoxydhCer
C20-Cer	C20-deoxyCer
C20-Cer	C20-deoxydhCer
C24:1-deoxyCer	C22:1-deoxyCer
C24:1-deoxydhCer	C22:1-deoxydhCer
C22-Cer	C22-deoxyCer
C22-Cer	C22-deoxydhCer
C24:1-deoxyCer	C24-deoxyCer
C24:1-deoxydhCer	C24-deoxydhCer
C24:1-deoxyCer	C26:1-deoxyCer
C24:1-deoxydhCer	C26:1-deoxydhCer
C24-Cer	C26-deoxyCer
C24-Cer	C26-deoxydhCer

Fig. 2.

Parameters of sphingolipid and deoxySL calculations. *A)* Each species of sphingolipid and deoxySL measured is listed along with its precursor ion, product ion, collision energy, and retention time. *B)* The source species were directly used for measurements of deoxySL targets.

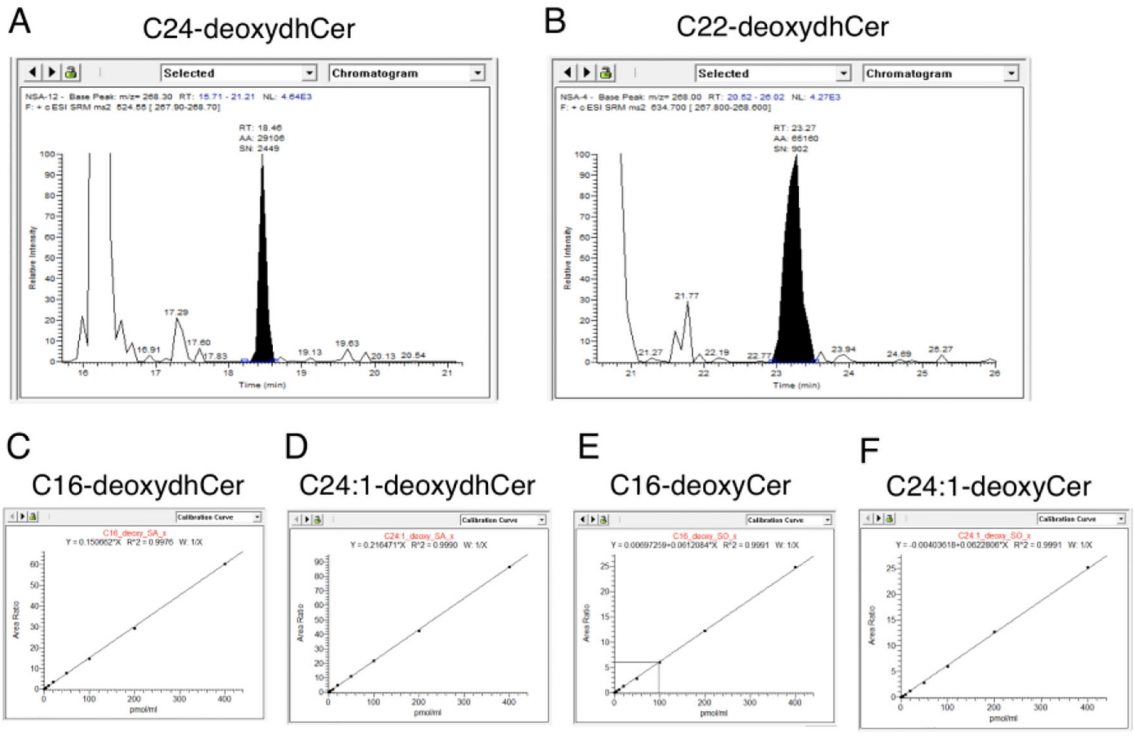

Fig. 3.

Verification of identified deoxySLs. *A-B)* Sample peaks provided for C24-deoxydhCer and C22-deoxydhCer, respectively, demonstrating a reliable signal to noise ratio. *C-F)* Calibration curves for C16-deoxydhCer, C24:1-deoxydhCer, C16-deoxyCer, and C24:1-deoxyCer demonstrating high linearity validating the method.

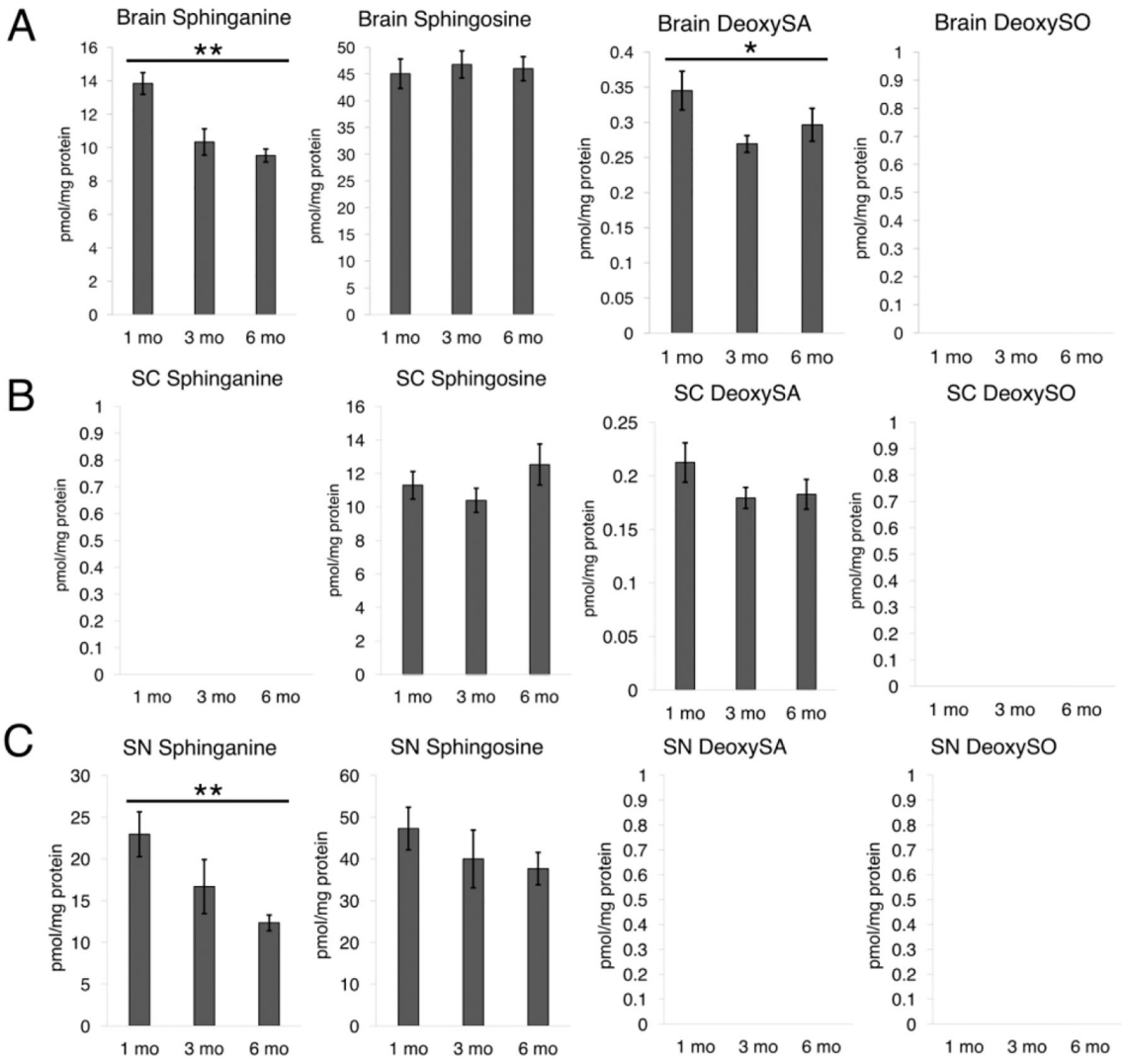

Fig. 4.

Sphingoid and deoxysphingoid base profiles in mouse neural tissue. *A)* Brain tissue from 1 month, 3 month, and 6 month mice analyzed for sphinganine, sphingosine, deoxySA, and deoxySO ($P = 0.0054, 0.8948, 0.0342$). Note that empty graphs with "BDL" indicate a species was below the detectable level of confident quantification. *B)* Spinal cord tissue analyzed as in 4A ($P = 0.5195, 0.1576$). *C)* Sciatic nerve analyzed as in 4A ($P = 0.0078, 0.2050$). $*P < 0.05$, $**P < 0.01$, $***P < 0.001$

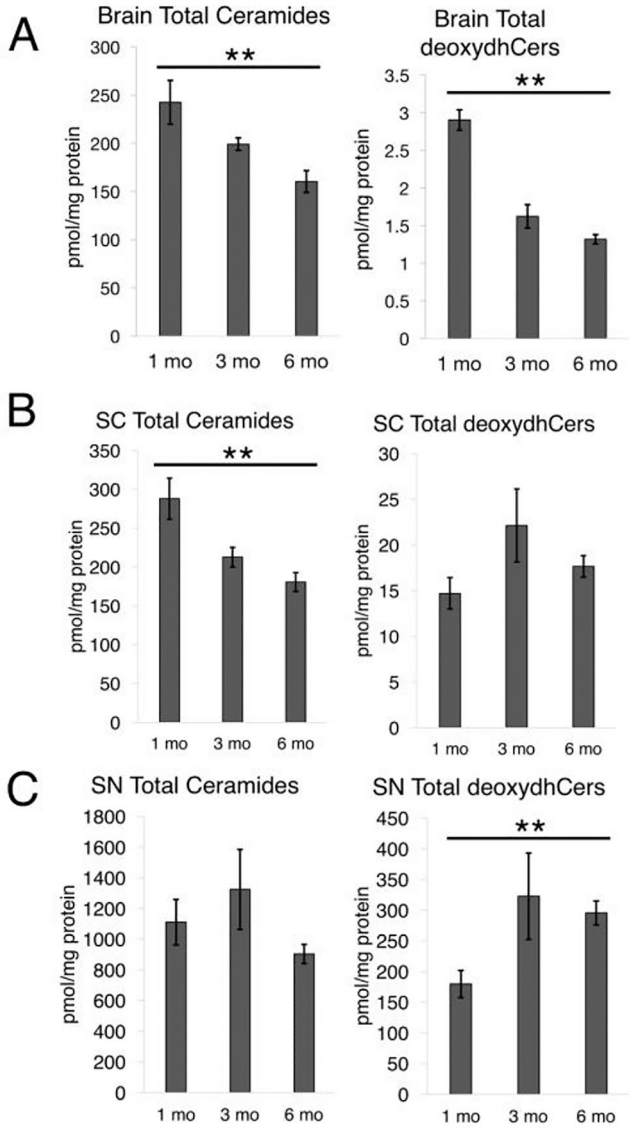

Fig. 5.

Cers and deoxydhCers in mouse neural tissue. *A)* Brain tissue from 1 month, 3 month, and 6 month mice analyzed for total Cer and total deoxydhCer ($P = 0.0059, 0.0019$). *B)* Spinal cord tissue analyzed as in 5A ($P = 0.0044, 0.3722$). *C)* Sciatic nerve analyzed as in 5A ($P = 0.0800, 0.0051$).

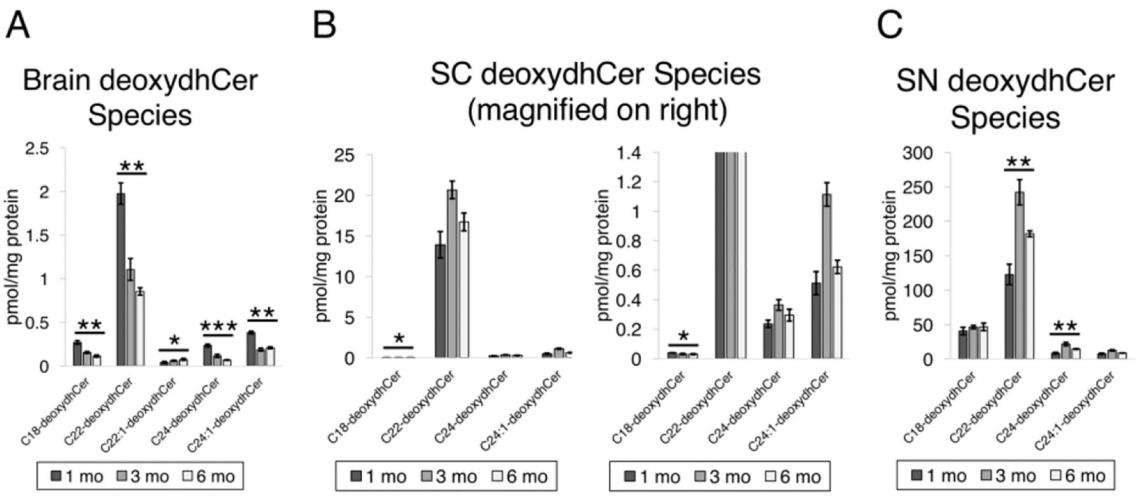

Fig. 6.

DeoxydhCer profile in mouse neural tissue. *A)* DeoxydhCer species that were measured from brain tissue from 1 month, 3 month, and 6 month mice (P = 0.0015, 0.0017, 0.0423, 0.0008, 0.0023). *B)* Spinal cord tissue analyzed as in 6A (P = 0.0142, 0.3722, 0.5195, 0.1641). Note multiple panels are presented to show relative levels of all species measured, including C22-deoxydhCer and those that are less prevalent. *C)* Sciatic nerve analyzed as in 6A (P = 0.3123, 0.0051, 0.0021, 0.1136).